

Coronal prominence cavities and forward modeling

Coronal mass ejections (CMEs) and associated prominence eruptions are spectacular manifestations of the Sun's magnetic energy. The genesis of these eruptions is both a fascinating physical puzzle and a key requirement for predicting and mitigating potentially hazardous space weather. Elliptical regions of rarefied density, or cavities, are commonly observed surrounding coronal prominences prior to their eruption. The prominence-cavity system is structured by magnetism, providing clues to the processes that destabilize these equilibria and drive CMEs. The 2008-2010 ISSI [International Team on Prominence Cavities](#) successfully undertook a broad observational analysis of prominence cavities in multiple wavelengths (from radio to soft X-ray to white light), and compared these to physical models. This work resulted in five publications to date, with two more in preparation, establishing for the first time measurements of large-scale line-of-sight flows in cavities, a three-dimensional model of cavity morphology, density and temperature properties of cavities in the low corona, and evidence for twisted magnetic flux rope fields within a cavity.

Our analyses were enabled by a suite of forward-modeling IDL codes that was written by members of the team. Solar coronal observables depend upon density, temperature, velocity, and magnetic field, all of which are important constraints on theoretical models. Comparing models to data is not always straightforward, however, since each observable depends on coronal plasma properties in different ways. Moreover, the optically-thin corona results in observables that are integrated along the line of sight. Such integrals can in some special cases be inverted (e.g., the work of Fuller and Gibson (2009)). A more general approach is to forward model – to take a model-defined three-dimensional distribution of coronal plasma properties, and perform line-of-sight integrals specific to a given coronal observable's dependence on these properties. Our team has constructed a [suite of forward modeling software](#) in IDL Solarsoft that enables side-by-side comparisons of model predictions and data. This “FORWARD tree” includes a set of magnetohydrodynamic models and is capable of reproducing a broad range of observables, from white light to EUV to coronal Stokes polarimetry parameters.

Related Publications

[Fuller and Gibson \(2009\)](#) used a Van de Hulst inversion of white-light polarized brightness (pB) data to study trends in density profiles for 24 cavity systems. The mean cavity density was over four times greater than that of a coronal hole at an altitude of $1.2 R_{\text{sun}}$ and possessed a mean depletion relative to their surrounding streamers of 28% at this altitude. The majority of cavities had essentially zero depletion (cavity versus streamer) at their tops. The exceptions were the two smallest cavities studied, which also possessed the largest average depletion of cavity vs. streamer. Lastly, large cavities tended to have wide aspect ratios, while smaller cavities had narrow aspect ratios. These measurements are important constraints on magnetohydrodynamics (MHD) and thermodynamic models of coronal cavities.

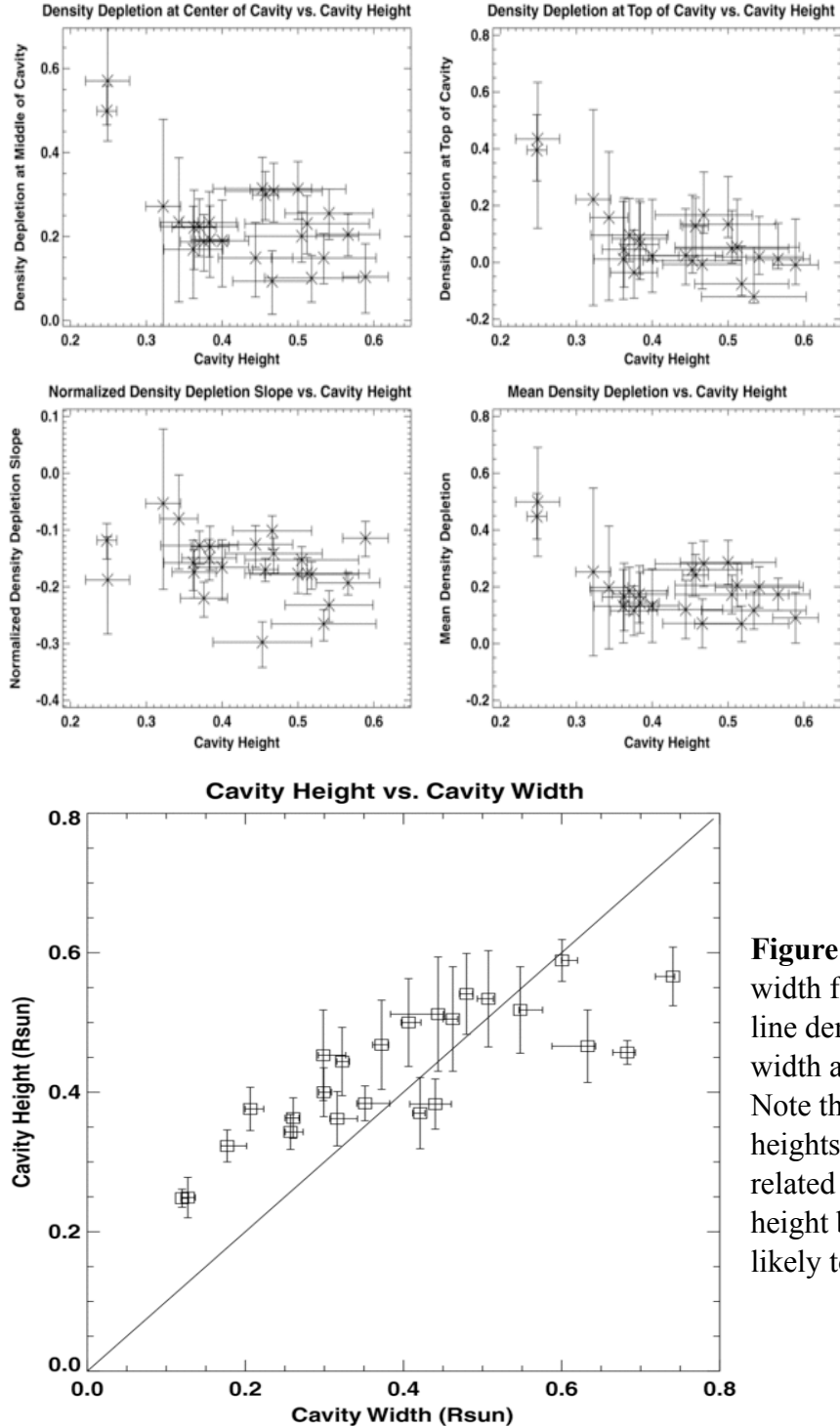
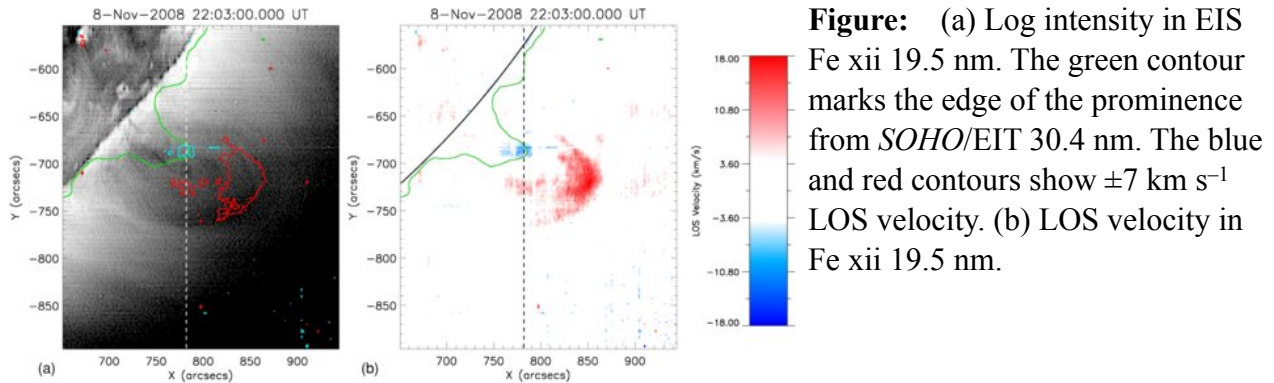
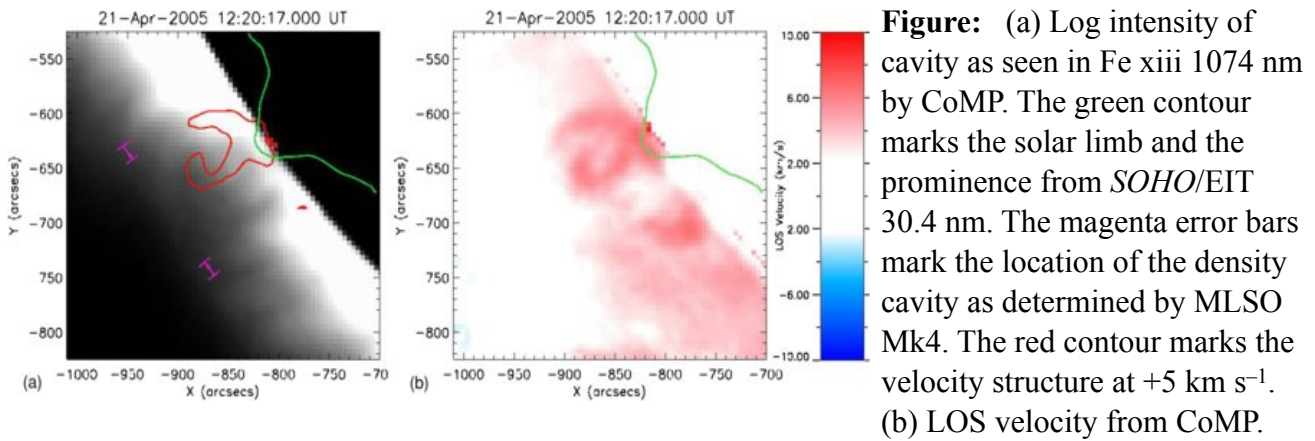


Figure: From top left: density depletion at the center of each cavity, density depletion at the top of each cavity, normalized density depletion slope (normalized so that height is measured as a fraction of cavity top height, rather than in absolute solar radius units), and mean density depletion of each cavity. The two smallest cavities appear to have quite different density properties, except in the plot of normalized density depletion. This may indicate self-similarity of cavity density distribution.

Figure: Cavity height vs. cavity width for our sample. The diagonal line denotes points where cavity width and cavity height are equal. Note the apparent asymptote of heights to 0.5 R_{sun} : this may be related to an upper limit on cavity height beyond which the structure is likely to erupt.

[Schmit et al. 2009](#) analyzed two different cavities, one observed by the Coronal Multichannel Polarimeter (CoMP) on 2005 April 21 and one by the Hinode Extreme ultraviolet Imaging Spectrometer (EIS) on 2008 November 8. Inside both of these cavities, coherent velocity structures were found as evidenced by spectral Doppler shifts. These flows had speeds of 5–10 km s^{-1} , occurred over length scales of tens of megameters, and persisted for at least one hour.

Flows in cavities are an example of the non-static nature of quiescent structures in the solar atmosphere. Moreover, they are evidence for a line-of-sight magnetic axis within the cavity.



[Gibson et al. \(2010\)](#) presented a three-dimensional density model of coronal prominence cavities, and a morphological fit that was tightly constrained by a uniquely well-observed cavity. Observations were obtained as part of an International Heliophysical Year campaign by instruments from a variety of space- and ground-based observatories, spanning wavelengths from radio to soft-X-ray to integrated white light. From these data it was clear that the prominence cavity was the limb manifestation of a longitudinally-extended polar-crown filament channel, and that the cavity was a region of low density relative to the surrounding corona. As a first step towards quantifying density and temperature from campaign spectroscopic data, the study established the three-dimensional morphology of the cavity. This is critical for taking line-of-sight projection effects into account, since cavities are not localized in the plane of the sky and the corona is optically thin. A global coronal streamer model was augmented to include a tunnel-like cavity with elliptical cross-section and a Gaussian variation of height along the tunnel length. A semi-automated routine was developed to fit ellipses to cross-sections of the cavity as it rotated past the solar limb, and was applied to Extreme Ultraviolet Imager (EUVI) observations from the two Solar Terrestrial Relations Observatory (STEREO) spacecraft. This defined the morphological parameters of the model, from which forward-modeled cavity observables could be reproduced. An important conclusion was that cavity morphology and

orientation, in combination with the viewpoints of the observing spacecraft, explained the observed variation in cavity visibility for the east vs. west limbs.

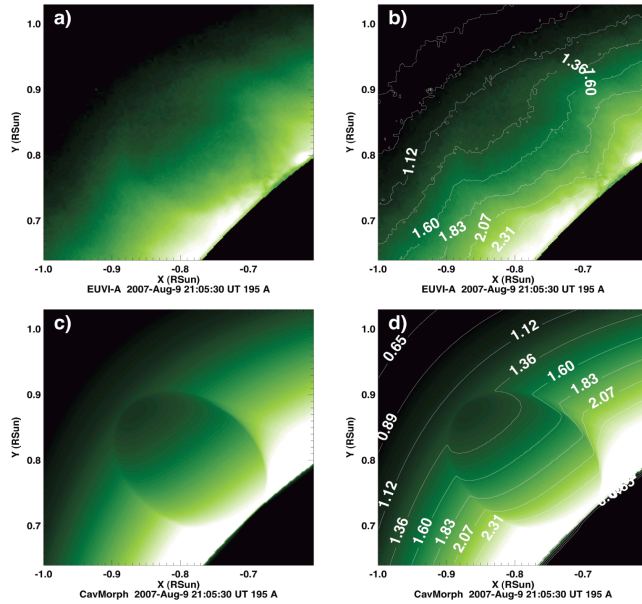


Figure: Forward modeling a coronal prominence cavity (Gibson et al., 2010). (a) STEREO EUVI-A image of the cavity with (b) intensity contours overlaid. (c) Forward modeled (line-of-sight integrated) EUV emission using model density and temperature with (d) intensity contours overlaid. Contours are in units of DN_s-1.

Building upon the 3D morphological cavity model of Gibson et al. (2010), **Schmit and Gibson (2011, submitted)** forward-modeled density-sensitive observables such as white light polarization brightness and the Fe XII 195.1 Å and 186.6 Å spectral line ratio for the cavity and its surrounding streamer. Then, via a genetic algorithm search of parameter space a best fit density model was established that matched observations from the Mauna Loa Solar Observatory Mk4 K-Coronameter and Hinode/EIS. The effect of temperature variations on the derived density was also measured, and densities established as a function of height in the cavity center $1.04 R_{\text{sun}}$ with height dependent error bars. This marked the first cavity density determination for the corona below $1.1 R_{\text{sun}}$, and demonstrated the usefulness of the genetic-algorithm-forward method as a complementary technique to traditional line-ratio diagnostics for diffuse off-limb coronal structures.

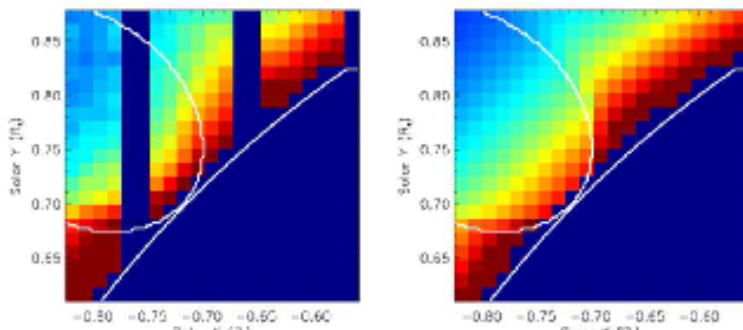


Figure: EIS line ratio image and synthetic line ratio based on the best fit isothermal density model. The plane-of-sky model cavity and the solar limb are marked by white lines. Both images use the same color table where blue is 0.04 and red is 0.16 in line ratio.

Dove et al. (Astrophys. Journ. Lett., 2011) found compelling evidence that prominence cavities are twisted magnetic flux ropes capable of storing the energy required to drive solar eruptions. For the first time, the CoMP instrument offers the capability of daily observations of the forbidden lines of Fe XIII with necessary spatial resolution and throughput to measure polarimetric signatures of current-carrying magnetohydrodynamic (MHD) systems. By forward-modeling CoMP observables from analytic MHD models of spheromak-type magnetic flux ropes, the predicted observable of such a flux rope oriented along the line of sight was demonstrated to be a bright ring of linear polarization surrounding a region where the linear polarization strength was relatively depleted. CoMP observations of the coronal cavity analyzed in Schmit et al. (2009) showed the presence of such a polarization ring.

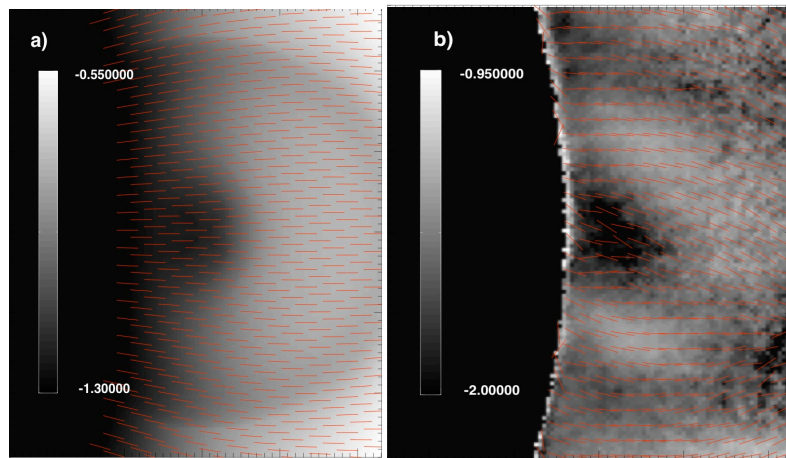


Figure. LOS-integrated Stokes linear polarization P/I for (a) forward-calculated spheromak configuration and (b) CoMP observations of April 21, 2005 southwest cavity. The range indicated by the color bar for (a) corresponds to 5–28% linear polarization, and for (b) corresponds to 1–11% linear polarization. Red lines indicate direction of P/I vectors.

References

- Fuller, J. and Gibson, S. E., A survey of coronal cavity density profiles. *ApJ*, 700, 1205, 2009
- Schmit, D., Gibson, S. E., Tomczyk, S., Reeves, K. K., Sterling, A., Brooks, D. and Tripathi, D., Large-scale flows in coronal cavities, *ApJL*, 700, 96, 2009
- Gibson, S. E., Kucera, T. A., Rastawicki, D., Dove, J., de Toma, G., Hao, J., Hill, S., Hudson, H. S., Marque, C., McIntosh, P. S., Rachmeler, L., Reeves, K. K., Schmieder, B., Schmit, D. J., Seaton, D. B., Sterling, A. C., Tripathi, D., Williams, D. R., Zhang, M., Three-dimensional morphology of a coronal prominence cavity, 724, 1133, *ApJ*, 2010
- Dove, J. B., Gibson, S. E., Rachmeler, L. A., Tomczyk, S., and Judge, P., Coronal magnometry: Observational signatures of magnetic flux ropes, *ApJ Letters*, accepted, 2011
- Schmit, D. J. and Gibson, S. E., Forward modeling cavity density: a multi-instrument diagnostic, submitted to *ApJ* 2011